Preparation and Properties of Polyurethane/Multiwalled Carbon Nanotube Nanocomposites by a Spray Drying Process

Wencai Wang,[1,2] Fengdan Jiang,[1,2]* Yi Jiang,[1,2] Yonglai Lu,[2,3] Liqun Zhang[1,3]

[1]*State Key Laboratory of Organic Inorganic Composites, Beijing 100029, China*
[2]*Key Laboratory of Carbon Fiber and Functional Polymers, Ministry of Education, College of Materials Science and Engineering, Beijing University of Chemical Technology, Beijing 100029, China*
[3]*Key Laboratory of Beijing City on Preparation and Processing of Novel Polymer Materials, Beijing 100029, China*

Received 23 May 2011; accepted 30 January 2012
DOI 10.1002/app.36936
Published online in Wiley Online Library (wileyonlinelibrary.com).

ABSTRACT: A spray drying approach has been used to prepare polyurethane/multiwalled carbon nanotube (PU/MWCNT) composites. By using this method, the MWCNTs can be dispersed homogeneously in the PU matrix in an attempt to improve the mechanical properties of the nanocomposites. The morphology of the resulting PU/MWCNT composites was investigated by scanning electron microscopy (SEM) and transmission electron microscopy (TEM). SEM and TEM observations illustrate that the MWCNTs are dispersed finely and uniformly in the PU matrix. X-ray diffraction results indicate that the microphase separation structure of the PU is slightly affected by the presence of the MWCNTs. The mechanical properties such as tensile strength, tensile modulus, elongation at break, and hardness of the nanocomposites were studied. The electrical and the thermal conductivity of the nanocomposites were also evaluated. The results show that both the electrical and the thermal conductivity increase with the increase of MWCNT loading. In addition, the percolation threshold value of the PU composites is significantly reduced to about 5 wt % because of the high aspect ratio of carbon nanotubes and exclusive effect of latex particles of PU emulsion in dispersion. © 2012 Wiley Periodicals, Inc. J Appl Polym Sci 000: 000–000, 2012

Key words: carbon nanotubes; polyurethane; mechanical properties; dynamic mechanical thermal analysis; conductivity

INTRODUCTION

Since the discovery of carbon nanotubes (CNTs) by Iijima in 1991,[1] they have attracted interest from scientists and engineers from all over the world. With unique and outstanding properties, such as excellent strength, modulus, electrical and thermal conductivities, and low density, CNTs have attracted much attention in the field of polymer/CNT composites.[2–7] Homogeneous dispersion of the CNTs in the polymer matrix and good interfacial bonding between the CNTs and the polymer matrix are the key factors affecting the properties of the composite. When compared with the enormous number of studies on the application of CNTs in epoxides, thermoplastics, and fibers, the number of reports dealing with the application of CNTs in elastomers was few because of the high viscosity of the elastomeric matrix.[8–11] Polyurethane (PU) is an important class of polymer materials for a variety of applications owing to their useful properties such as excellent flexibility, elasticity, and damping ability. The PU properties can be easily tailored through changing the molecular chain structures of the soft and hard segments. Therefore, it is reasonable to believe that PU can serve as an excellent matrix for polymer/CNTs. The CNT/elastomer nanocomposites could have broader application potential because of their unique mechanical, thermal, and electrical properties.

Traditional methods used for the preparation of polymer/CNT composites include melt blending,[12–15] *in situ* polymerization,[16–18] and solution methods.[19,20] However, in most of the studies, the incorporation of CNTs did not result in the expected reinforcement because the lack of chemical compatibility between the two phases led to poor dispersion of CNTs. Chemical modification of CNTs is regarded as an effective way of achieving well-dispersed CNTs in a polymer matrix[21,22]; however, chemical modification will inevitably result in the

**Present address:* China National Bluestar (Group) Co. Ltd.
Correspondence to: L. Q. Zhang (zhanglq@mail.buct.edu.cn).
Contract grant sponsor: National Basic Research Program of China; contract grant number: 2011CB932603.
Contract grant sponsor: Natural Science Foundation of China; contract grant number: 51073013.
Contract grant sponsor: State Key Laboratory of Polymer Materials Engineering, Sichuan University; contract grant number: KF200902.
Contract grant sponsor: Program for New Century Excellent Talents in University (NCET-11-0562).

disruption of the tube structure and loss in superior properties of the CNTs. Powder–rubber composites reinforced with CNTs by means of spray drying[23] has proved that the novel technology is better than the traditional methods for preparing CNT-reinforced elastomer composites with high viscosity.

In this work, we prepared PU/MWCNT composites by a spray drying process. The MWCNTs were well dispersed in the PU matrix as revealed by scanning electron microscopic (SEM) and transmission electron microscopic (TEM) images. The mechanical properties, electrical conductivity, and thermal conductivity of the composites were characterized.

EXPERIMENTAL

Materials

Waterborne PU was purchased from Beijing Jinhuili Applied Chemical Products, with a solid content of 30 wt %. MWCNTs with purity of 95 wt % were prepared by chemical vapor deposition and were supplied by Tsinghua University, China. The diameter and the length of the MWCNTs were in the ranges 10–20 nm and 0.5–1000 μm, respectively. Sodium dodecyl sulfonate (SDS) used as a dispersant was obtained from Sinopharm Chemical Reagent.

Preparation of PU/MWCNT composites

The pristine MWCNTs were mixed with SDS in a mass ratio of 10 : 1, and the mixture was added into deionized water. After supersonic stirring, a suspension of MWCNTs was obtained. Different amounts (0, 1, 3, 5, 10, and 20 phr) of the above suspension were mixed with 100 phr PU. Deionized water was gradually added to each mixture, and a suspension of MWCNTs in the PU latex was obtained after dispersion in an ultrasonic processor for 3 h. A mixed PU/CNTs latex suspension with a total solid content of about 10 wt % was obtained. The above MWCNT–PU latex suspension was sprayed and dried by a spraying dryer (Model B290; Büchi, Switzerland). The spray condition was as follows: air inlet temperature of 160°C, suspensions feeding rate of 200 mL h^{-1}, and a nozzle cleaner of 4 min^{-1}. The spray dry process is schematically shown in Figure 1.

Finally, the PU/MWCNT composites were compressed to slices of 10 cm × 15 cm in size by using a hot press at 180°C under 15 MPa for 10 min and then cold pressed at room temperature under 15 MPa.

Characterization

The fracture morphology of the PU/MWCNT composites was investigated by an XL-30 field-emission SEM produced by FEI. The SEM specimens were prepared by free fracturing under cryogenic conditions, and then gold particles were sprayed on the surface of the specimens. The morphology of the PU/MWCNT composites was observed by an H-800 TEM produced by Hitachi, Japan. The specimens for TEM observations were prepared by cryogenic microtoming with a Reicherte Jung Ultracut Microtome and mounted on 200-mesh copper grids.

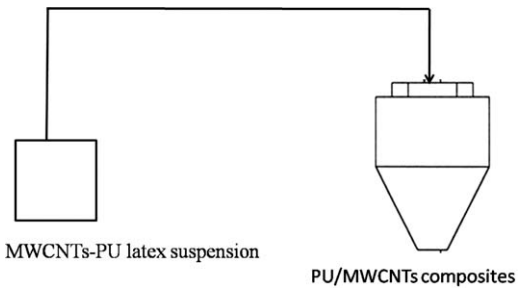

Figure 1 Schematic illustration of the preparation process for PU/MWCNT composites.

X-ray diffraction (XRD) studies were carried out in the 2θ range of 5°–90° by using a Rigaku D/Max 2500VBZt/PC X-ray diffractometer (Rigaku, Japan). The scanning speed was 0.02° s^{-1}.

The "Payne effect" of the composites was measured at 170°C and 1 Hz as a function of strain amplitude in the range 0–400% by using a Monsanto RPA-2000 apparatus (Monsanto, St. Louis, MO).

The shore A hardness of the composites was measured according to ASTM D-2240 by using an XY-1 type A durometer (No. 4 Chemical Machinery Plant of Shanghai Chemical Equipment, Shanghai, China). Three different locations of the same sample (>6 mm in thickness) were measured to get an average value.

Tensile tests of dumbbell specimens were carried out on a CMT4104 testing machine (Shenzhen SANS Testing Machine, Shenzhen, China) at a speed of 500 mm min^{-1}, according to ASTM D-412. The storage modulus, loss modulus, and tan δ were measured as a function of temperature with dynamic mechanical thermal analysis (DMTA VA3000; Rheometric Scientific, NJ, USA) in the tension mode at a frequency of 10 Hz and temperature increments of 3°C min^{-1}.

The electrical conductivity of the PU/MWCNT composites was measured by using a digital multimeter when the resistance was below 2×10^7 Ω and a ZC43-type megger when the resistance was above 2×10^7 Ω. The thermal conductivity of the PU/MWCNT composites was measured by a heat flow meter (FOX50, Laser Comp., MA, USA).

RESULTS AND DISCUSSION

Morphology of PU/MWCNT composites

The fracture morphology of the PU/MWCNT composites with different MWCNT loadings are shown in Figure 2. As can be seen in Figure 1, MWCNTs

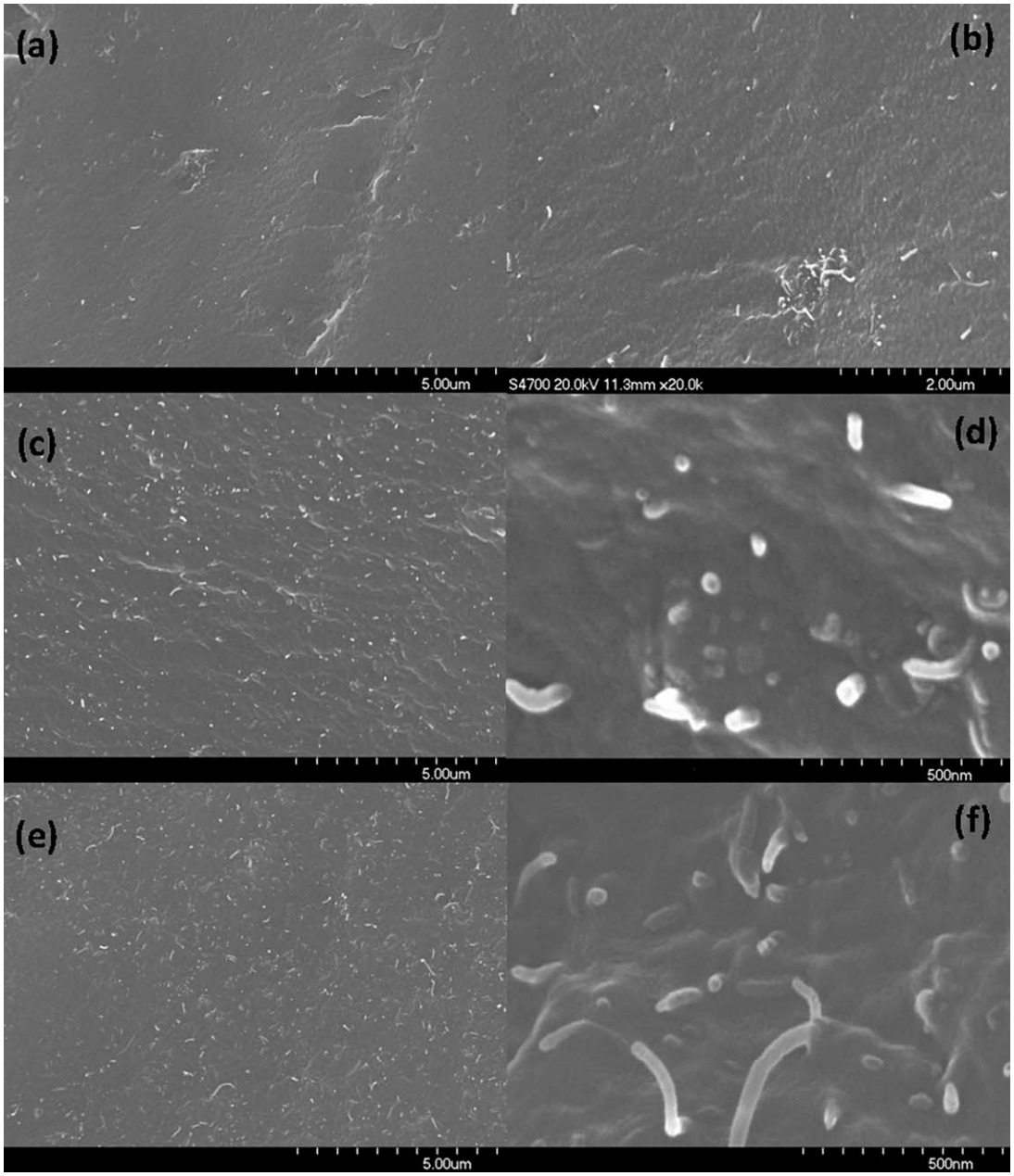

Figure 2 SEM images of PU/MWCNT composites with different MWCNT loadings: (a and b) 1 phr; (c and d) 5 phr; and (e and f) 10 phr.

are well dispersed in the PU matrix regardless of the MWCNT loading. The good dispersion was further confirmed by the representative TEM images of the PU/MWCNT composites shown in Figure 3. The PU emulsion was dispersed by the ultrasonic method, and the suspension was dried quickly by the spray drying process, both processes preventing MWCNTs from aggregating in the PU matrix. In addition, there were many outcrops of broken MWCNTs on the fractured surfaces of the PU/MWCNT composites [Fig. 2(d,f)], indicating a strong interaction between the MWCNTs and the PU matrix. It indicates that the MWCNTs suffered some mechanical loads during the tensile test.

XRD patterns of PU/MWCNT composites

Figure 4 shows the XRD patterns for PU, MWCNTs, and PU/MWCNT composites. The PU clearly shows a strong diffraction peak at $2\theta = 17.5^\circ$, whereas the MWCNTs show two diffraction peaks at $2\theta = 25.6^\circ$ and 42.8°, which correspond to different crystallite species of crystalline graphite. The locations of the above three peaks remain the same in the pattern

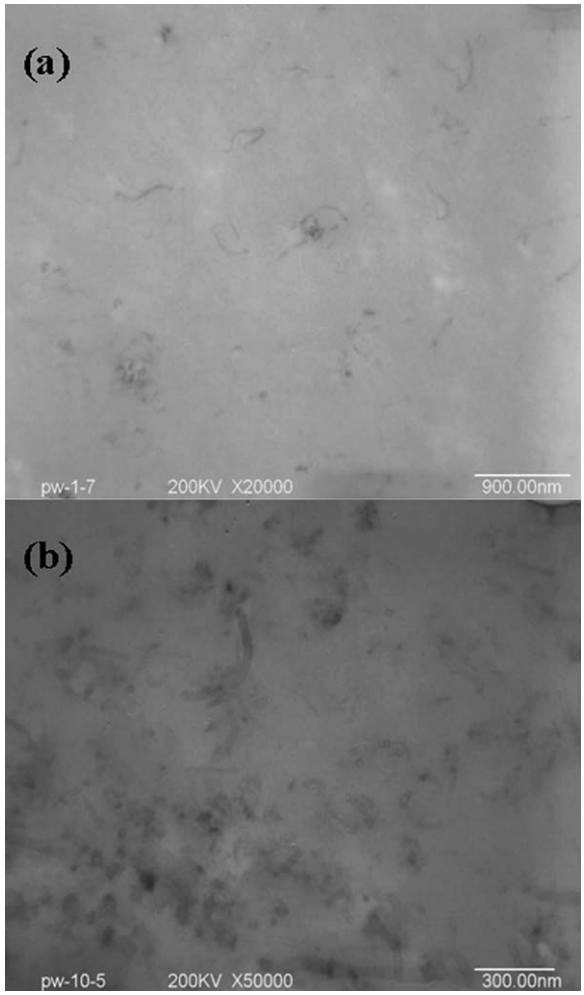

Figure 3 TEM images of PU/MWCNT composites with different MWCNT loadings: (a) 1 phr and (b) 10 phr.

for PU/MWCNT composites, indicating that the introduction of MWCNTs did not affect the microstructure of PU.

Dynamic mechanical properties of PU/MWCNT composites

The effect of MWCNT loading on the dynamic mechanical properties of composites was analyzed by DMTA in this work. The elastic modulus (E') and the loss factor (tan δ) of the pristine PU and PU/MWCNT composites are plotted as a function of temperature in Figure 5. Under an oscillating force, the resultant strain on the specimen depends on both the elastic and the viscous behavior of the material. The storage modulus is a measure of the recoverable strain energy in a deformed specimen and reflects the elasticity of the material, and the loss factor is related to damping as a result of energy dissipation.

Figure 5(a) shows that the storage modulus of the PU/MWCNT composites is higher than that of the pristine PU at all temperatures and that the storage modulus increases with increasing MWCNT loading. The high modulus and specific surface area of MWCNTs enhance the stiffness of the PU, resulting in an increase of storage modulus of the PU/MWCNT composites. The CNT network will lead to stress transfer, as well as hindrance of plastic flow for the PU/MWCNT composites, resulting in the increase in the stiffness of PU. At low temperatures, the modulus of the pristine PU is high because of the semicrystalline characteristic of PU, and the addition of MWCNTs has little effect on the modulus. With the increase in the temperature, the E' of all specimens decreases. However, it is evident that the stiffness of PU increases as a result of the addition of MWCNT, and the stiffness increased with the increment of with MWCNT loading. Therefore, the transition temperature (from rubbery state to viscous flow state) increases with increasing MWCNT loading, and the reinforcing effect is higher above the T_g of the composites.

As the temperature reached about 90°C, the hard phase of the pristine PU started to dissociate. The modulus of the PU quickly decreased because the physical crosslinks in the PU were destroyed. As a result, the PU changed into the viscous state. However, this modulus decay was greatly suppressed by the incorporation of MWCNTs and the elastic state persisted at higher temperatures. Therefore, the PU/MWCNT composites could keep a high modulus at high temperatures. This result was attributed to the nanotube–nanotube network structure, which increased the elasticity of the composites and prevented the composites from flowing under small deformations. Correspondingly, the loss factor of the PU/MWCNT composites at 200°C decreased with increasing MWCNT loadings because of both volume effect and interfacial interaction effect, as shown in Figure 5(b).

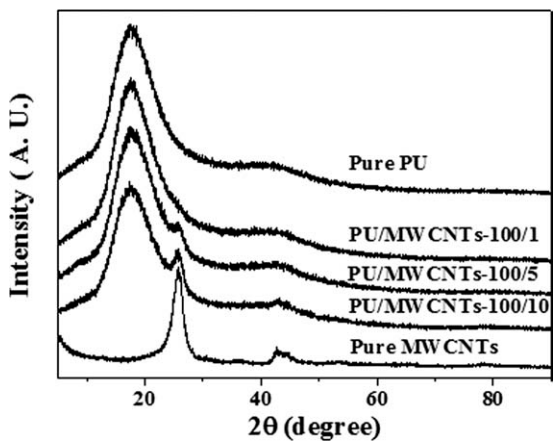

Figure 4 X-ray diffraction patterns of PU, MWCNT, and PU/MWCNT composites with different MWCNT loadings.

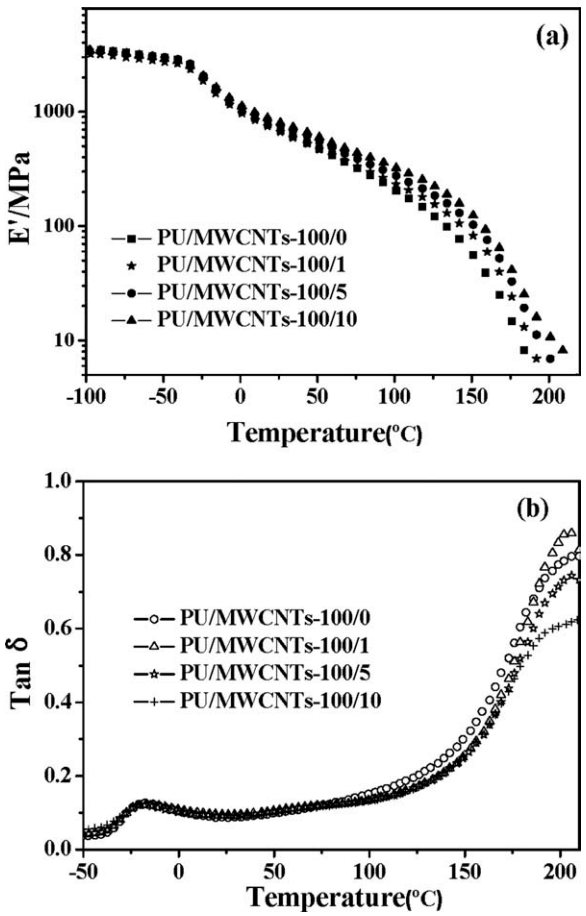

Figure 5 (a) Dynamic storage modulus and (b) loss factor as a function of temperature for pristine PU and PU/MWCNT composites.

Payne effect

At a given frequency and temperature, the shearing storage modulus (G') of unfilled rubbers is independent of the deformation amplitude. In contrast, G' for the filled rubber shows a significant dependency on the dynamic deformation; here, the value considerably decreases with the increment of strain amplitude. This nonlinear behavior of filled rubbers is known as the Payne effect[24,25] and has been explained by the existence of a filler network in the rubber matrix. With increasing strain amplitude, the filler network is breaking down, thus resulting in a decrease of the storage modulus.

Figure 6 shows the Payne effect of PU and PU/MWCNT composites with different MWCNT loadings. The plateau region is long for pristine PU, indicating that the dynamic modulus did not change with the increment of strain in a certain strain range. The decrease of modulus at high amplitudes of deformation was due to the disentanglement of macromolecule chains. With the increase of amplitude of deformation, the breakdown of the MWCNTs network leads to a rapid decrease of the storage modulus of the PU/MWCNT composites. When the amplitude of deformation was sufficiently large, the MWCNTs network was broken down completely and the storage modulus was reduced to a minimum. The higher the MWCNT loading, the higher is the degree of crosslinking network before breakdown. Therefore, the storage modulus at low amplitudes of deformation is higher, and the strain at which the storage modulus begins to decrease is smaller. The Payne effect increases with increasing MWCNT loadings.

Mechanical properties

The results of the mechanical properties testing are displayed in Table I. It can be seen that with the increase of MWCNT loading, the elongation at break decreased, the hardness of the composites increased gradually, and the tensile strength first decreased and then increased slowly. The above results are similar to the mechanical properties of short fiber/rubber composites.[26] Thermoplastic PU is a type of polymer with soft segment and hard segments. Small MWCNT loadings lead to an impurity effect and disrupt the order of soft and hard segments, leading to a decrease of tensile strength. When the MWCNT loading increased to 5 phr, the MWCNTs formed a network structure to which stress can be transferred from the PU matrix to offset the impurity effect. However, whether the tensile strength of the composites can exceed that of the pristine PU depends on the orientation and the aspect ratio of the MWCNTs and the interaction between MWCNTs and PU.

Functional properties

It has been recognized that MWCNT is an excellent reinforcing filler for the enhancement of physical and mechanical properties of polymer materials. Recently, a large amount of research work has focused on the functional properties of the polymer/MWCNT composites and properties brought about by the MWCNTs such as electrical conductivity[27–29] and thermal conductivity.[30,31] The percolation theory

TABLE I
Mechanical Properties of PU/MWCNT Composites with Different MWCNT Loadings

MWCNT loadings (phr)	Shore A hardness	Tensile strength (MPa)	Elongation at break (%)	Modulus at 100% elongation (MPa)
0	74	27.1	156	25.9
1	78	23.5	65	–
5	80	26.3	61	–
10	82	26.7	64	–

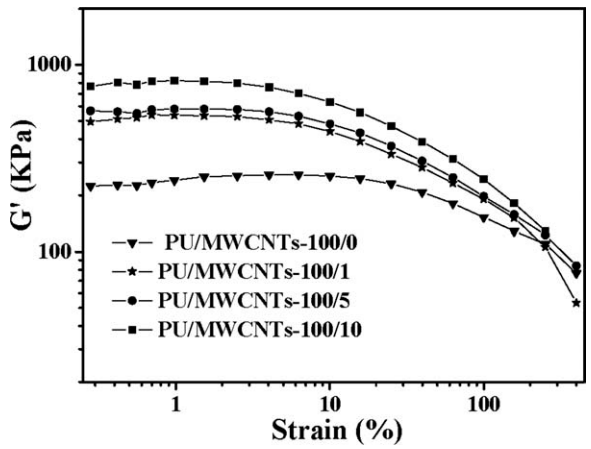

Figure 6 Payne effect and storage modulus versus deformation of PU/MWCNT composites with different MWCNT loadings.

has usually been used to explain the improvement in electrical conductivity of polymer/MWCNT composites, and the critical concentration of the fillers in the composite is called the percolation threshold.

Figure 7 shows the electrical conductivity and the thermal conductivity of the composites plotted against the MWCNT loading. The electrical conductivity did not show a significant increase when the MWCNT loadings increased from 0.5 to 4.5 wt %. The conductivity of the composites increased rapidly when the MWCNT loading exceeded 4.5 phr, and the conductivity reached a stable value at a MWCNT loading of 5.5 wt %. At a 5.5 wt % loading of MWCNTs, the electrical conductivity of the composite was 5×10^{-5} S cm^{-1}, an improvement of 11 orders of magnitude over that of pristine PU (9.7×10^{-16} S cm^{-1}). The percolation threshold of about 5 wt % is far smaller than the value of 10 wt % for PU/MWCNT composites prepared by melt blending.[32] Generally, the percolation threshold is related to the dispersity, orientation, and aspect ratio of the fillers. When the MWCNT loading is 10 phr, the degree of MWCNTs network is high, and it is beneficial to the formation of conductive paths. Therefore, the PU/MWCNT composites prepared by spray drying have the same aspect ratio of MWCNTs as that of composites prepared by melt blending, which is also beneficial to the formation of conductive paths. A possible explanation is that the expected maximum conductivity of the single tubes (about 10^4 S cm^{-1}) is by far not reached for the PU/MWCNT composites above the percolation threshold in the electrical measurements. In fact, Figure 7(a) shows a plateau value of about 10^{-2} S cm^{-1}, which lies about six orders of magnitudes below that of the single tubes. This result clearly demonstrates that the charge transport through the tube network embedded in the PU matrix is hindered strongly by quantum tunneling effects.

The improvement in thermal conductivity is another focus on the polymer/CNT composites because of the superior thermal conductivity of CNTs. It has been experimentally shown that the thermal conductivity of polymers was slightly enhanced by the incorporation of CNTs.[33,34] Figure 7(b) shows the thermal conductivity of PU/MWCNT composites plotted against the MWCNT loading. These results show that the thermal conductivity increases gradually with the increase of MWCNT loading. At 8 wt % loading of MWCNTs, the thermal conductivity of the composite is 0.27 W m^{-1} K^{-1}, which is 1.69 times that of pristine PU (0.16 W m^{-1} K^{-1}). Obviously, when compared with the phenomena shown in Figure 7(a), the effect of MWCNTs on the thermal conductivity is not obvious. The presence of gaps in the MWCNTs network is expected to limit the transport of charge carrier significantly, leading to a strong reduction of thermal conductivity induced by electron transport. For MWCNTs dispersed in a polymer matrix, further scattering effects such as interfacial boundary scattering and defect scattering will appear, leading to a drastic reduction of thermal transport properties.[35] In addition, the thermal transport through the MWCNTs network by

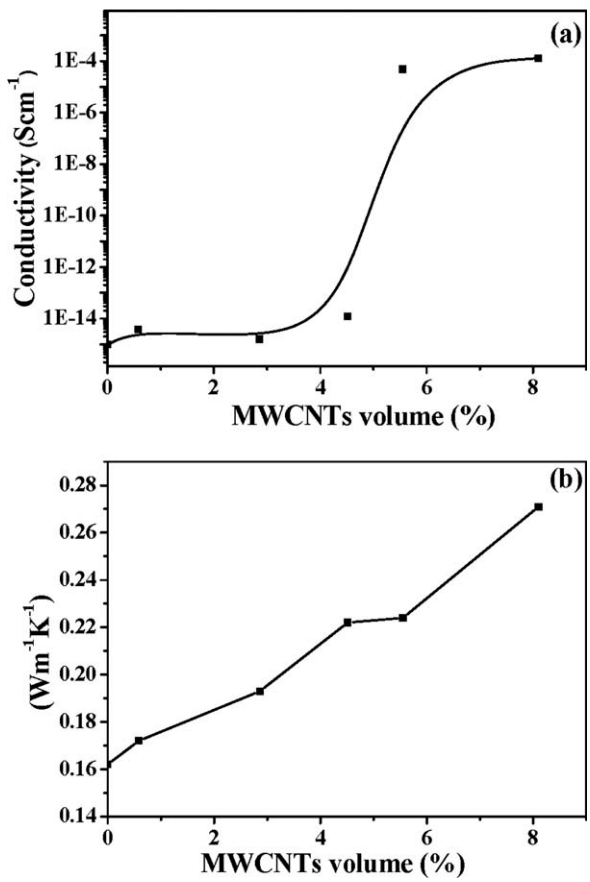

Figure 7 (a) Electrical conductivity and (b) thermal conductivity of PU/MWCNT composites with different MWCNT loadings.

phonons will be strongly hindered by the gaps between adjacent tubes. Thus, it is not surprising that the thermal conductivity of the PU/MWCNT composites is several orders of magnitude below than that of the isolated MWCNTs (up to 3000 W m^{-1} K^{-1}). Furthermore, the percolation behavior, as observed for the electrical conductivity [Fig. 7(a)], is not found in Figure 7(b). This is mainly due to the difference in the mechanism of electrical and thermal conductivities. In electrical conductivity, the electrons transport through the CNTs. However, the phonons may be transferred not only through the CNTs but also through the CNT to the PU matrix. As a result, the increase of thermal conductivity does not show a percolation threshold with the increase of CNT loading.

CONCLUSIONS

PU/MWCNT nanocomposites were successfully prepared by a spray drying process. SEM and TEM images showed that the MWCNTs were well dispersed in the PU matrix. With the increase of the MWCNT loading, the modulus of the PU/MWCNT composites increased and the thermal stability improved. The electrical conductivity results revealed the presence of a percolation network at filler loadings as low as 5 wt %. The electrical conductivity of the composites was improved by more than 11 orders of magnitude with the addition of 5.5 wt % MWCNTs. The incorporation of MWCNTs into PU resulted in only a slight enhancement of the thermal conductivity. The theoretically predicted thermal conductivity of isolated tubes of MWCNTs cannot be realized in PU-based composites in practice. Obviously, the large surface area of the CNTs leads to strong phonon boundary scattering, which results in poor thermal conductivity.

References

1. Iijima, S. Nature 1991, 354, 56.
2. Thostenson, E. T.; Ren, Z. F.; Chou, T. W. Compos Sci Technol 2001, 61, 1899.
3. Coleman, J. N.; Khan, U.; Gun'ko, Y. K. Adv Mater 2006, 18, 689.
4. Tang, B. Z.; Xu, H. Y. Macromolecules 1999, 32, 2569.
5. Liff, S. M.; Kumar, M.; McKinley, G. H. Nat Mater 2007, 6, 76.
6. Sahoo, N. G.; Jung, Y. C.; Yoo, H. J.; Cho, J. W. Macromol Chem Phys 2006, 207, 1773.
7. Fernández-d'Arlas, B.; Khan, U.; Rueda, L.; Coleman, J. N.; Mondragon, I.; Corcuera, M. A.; Eceiza, A. Compos Sci Technol 2011, 71, 1030.
8. Bokobza, L. Polymer 2007, 48, 4907.
9. López-Manchado, M. A.; Biagiotti, J.; Valentini, L.; Kenny, J. M. J Appl Polym Sci 2004, 92, 3394.
10. Kim, Y. A.; Hayashi, T.; Endo, M.; Gotoh, Y.; Wada, N. J Scr Mater 2006, 54, 31.
11. Frogley, M. D.; Ravich, D.; Wagner, H. D. Compos Sci Technol 2003, 63, 1647.
12. Potschke, P.; Fornes, T. D.; Paul, D. R. Polymer 2002, 43, 3247.
13. Seo, M. K.; Park, S. J. Chem Phys Lett 2004, 395, 44.
14. López-Manchado, M. A.; Valentini, L.; Biagiotti, J.; Kenny, J. M. Carbon 2005, 43, 1499.
15. Wang, M.; Pramoda, K. P.; Goh, S. Carbon 2006, 44, 613.
16. Xia, H.; Wang, Q.; Qiu, G. Chem Mater 2003, 15, 3879.
17. Yang, Z.; Dong, B.; Huang, Y.; Liu, L.; Yan, F. Y.; Li, H. L. Mater Chem Phys 2005, 94, 109.
18. Zeng, H.; Gao, C.; Wang, Y.; Watts, P. C. P.; Kong, H.; Cui, X.; Yan, D. Polymer 2006, 47, 113.
19. Sluzarenko, N.; Heurtefeu, B.; Maugey, M.; Zakri, C.; Poulin, P.; Lecommandoux, S. Carbon 2006, 44, 3207.
20. Sung, Y. T.; Han, M. S.; Song, K. H.; Jung, J. W.; Lee, H. S.; Kum, C. K.; Joo, J.; Kim, W. N. Polymer 2006, 47, 4434.
21. Xia, H.; Song, M.; Jin, J.; Chen, L. Macromol Chem Phys 2006, 207, 1945.
22. Kim, J. A.; Seong, D. G.; Kang, T. J.; Youn, J. R. Carbon 2006, 44, 1898.
23. Wang, J. D.; Zhu, Y. F.; Zhou, X. W.; Sui, G.; Liang, J. J Appl Polym Sci 2006, 100, 4697.
24. Payne, A. R.; Wittaker, R. E. Rubber Chem Technol 1971, 44, 3.
25. Heinrich, G.; Klüppel, M. Adv Polym Sci 2002, 160, 1.
26. Zhang, L. Q.; Jin, R. G.; Geng, H. P.; Chen, S.; Zhou, Y. H. Acta Mater Compos Sinica 1998, 15, 89.
27. Wang, Z.; Lua, M.; Li, H. L.; Guo, X. Y. Mater Chem Phys 2006, 100, 77.
28. Li, Z.; Luo, G.; Wei, F.; Huang, Y. Compos Sci Technol 2006, 66, 1022.
29. Pötschke, P.; Bhattacharyya, A. R.; Janke, A. Polymer 2003, 44, 8061.
30. Berber, S.; Kwon, Y. K.; Tománek, D. Phys Rev Lett 2000, 84, 4613.
31. Yang, D. J.; Wang, S. G.; Zhang, Q.; Sellin, P. J.; Chen, G. Phys Lett A 2004, 329, 207.
32. Jiang, F. D.; Wu, S. Z.; Wei, Y. J.; Zhang, L. Q.; Hu, G. H. Polym Compos 2008, 16, 471.
33. Kashiwagi, T.; Grulke, E.; Hilding, J.; Groth, K.; Harris, R.; Butler, K.; Shields, J.; Kharchenko, S.; Douglas, J. Polymer 2004, 45, 4227.
34. Xia, H.; Song, M. Soft Matter 2005, 1, 386.
35. Gojny, F. H.; Wichmann, M. H. G.; Fiedler, B.; Kinloch, I. A.; Bauhofer, W.; Windle, A. H. Polymer 2006, 47, 2036.